Society For Biomaterials

Comparison of the effects of 45S5 and 1393 bioactive glass microparticles on hMSC behavior

Taimoor H. Qazi,[1,2] Shahzad Hafeez,[1,3]* Jochen Schmidt,[4] Georg N. Duda,[1,2,5] Aldo R. Boccaccini,[3] Evi Lippens[1,2]

[1]Julius Wolff Institut, Charité, Universitätsmedizin Berlin, Berlin, 13353, Germany
[2]Berlin-Brandenburg School for Regenerative Therapies, Charité, Universitätsmedizin Berlin, Berlin 13353, Germany
[3]Institute of Biomaterials, Department of Materials Science and Engineering, University of Erlangen-Nuremberg, Erlangen 91058, Germany
[4]Institute of Particle Technology, University of Erlangen-Nuremberg, Erlangen 91058, Germany
[5]Berlin-Brandenburg Center for Regenerative Therapies, Charité, Universitätsmedizin Berlin, Berlin 13353, Germany

Received 23 January 2017; revised 22 May 2017; accepted 26 May 2017
Published online 6 July 2017 in Wiley Online Library (wileyonlinelibrary.com). DOI: 10.1002/jbm.a.36131

Abstract: Bioactive glasses (BAGs) are highly interesting materials for bone regeneration applications in orthopedic and dental defects. It is quite well known that ionic release from BAGs influences cell behavior and function. Mindful of the clinical scenario, we hypothesized that local cell populations might additionally physically interact with the implanted BAG particles and respond differently than to just the ionic stimuli. We therefore studied the biological effect of two BAG types (45S5 and 1393) applied to human mesenchymal stromal cells (hMSCs) in three distinct presentation modes: (a) direct contact; and to dissolution products in (b) 2D, and (c) 3D culture. We furthermore investigated how the dose-dependence of these BAG particles, in concentrations ranging from 0.1 to 2.5 w/v %, influenced hMSC metabolic activity, proliferation, and cell spreading. These cellular functions were significantly hampered when hMSCs were exposed to high concentrations of either glasses, but the effects were more pronounced in the 45S5 groups and when the cells were in direct contact with the BAGs. Furthermore the biological effect of 1393 BAG outperformed that of 45S5 BAG in all tested presentation modes. These outcomes highlight the importance of investigating cell–BAG interactions in experimental set-ups that recapitulate host cell interactions with BAG particles. © 2017 Wiley Periodicals, Inc. J Biomed Mater Res Part A: 105A: 2772–2782, 2017.

Key Words: bioactive glass, hMSCs, microparticles, cell function, ion release

How to cite this article: Qazi TH, Hafeez S, Schmidt J, Duda GN, Boccaccini AR, Lippens E. 2017. Comparison of the effects of 45S5 and 1393 bioactive glass microparticles on hMSC behavior. J Biomed Mater Res Part A 2017:105A:2772–2782.

INTRODUCTION

With the discovery of 45S5 Bioglass® (45 SiO_2-24.5 CaO-24.5 Na_2O-6 P_2O_5 in wt. %) a new class of bioactive ceramic materials was created, characterized by their ability to form a strong and stable chemical bond with bone tissue.[1] Bioactive glasses (BAGs) have since attracted immense interest in the field of tissue engineering because of their demonstrated osteoconductive (stimulation of bone growth along its surface) and osteostimulatory (activation of osteoprogenitor cells in the bone environment) properties.[2] Additionally, BAGs facilitate the formation of a carbonated hydroxyapatite layer on their surface when exposed to biological fluids, and resorb over time.[3] Various *in vivo* studies have reported on the stimulatory effects of BAGs on bone healing—ranging from the regeneration of cranial defects in pre-clinical models[4] to the successful treatment of challenging bone defects in humans.[5]

Since the earlier studies performed by Xynos et al.[6] numerous reports have highlighted the important role of ionic dissolution products of BAGs in the induction of genes relevant to cellular function, particularly those responsible for osteoblast metabolism, bone homeostasis, and angiogenesis.[7–10] Thus, various types of BAGs have been developed with tailored chemical compositions and fine-tuned ion release kinetics to harness distinct biological processes.[11,12] This has opened a whole new exciting field of research of cell stimulation by synthetic materials without the need for organic growth factors.[13] Furthermore, mesoporous silica based glasses can be produced as micron and submicron sized SiO_2-CaO or SiO_2-CaO-P_2O_5 particles for the storage of signaling molecules and their localized release at the implantation site.[14] The design of bioactive glass structures with nano to micro scale dimensions results in an increase in the glasses'

Additional Supporting Information may be found in the online version of this article.
The authors acknowledge financial support from the European Union (H2020-NMP6-2015 - grant number 685872, MOZART), DFG (German Research Foundation—grant number DU298/18.1) and the Berlin-Brandenburg School for Regenerative Therapies.
Correspondence to: A. R. Boccaccini and E. Lippens; e-mails: evi.lippens@charite.de and aldo.boccaccini@ww.uni-erlangen.de
**Present address:* MERLN Institute for Technology Inspired Regenerative Medicine, Universiteitssingel 40, 6229 ER Maastricht, The Netherlands

bioactivity and enables the loading of therapeutic biomolecules to further stimulate the tissue regeneration process.[15,16]

Today, different classes of silicate BAGs are available on the market for clinical applications such as NovaBone, Biogran® and Perioglas which are based on the 45S5 Bioglass® composition. Also, BonAlive® (S53P4: 53 SiO_2-20 CaO-23 Na_2O-4 P_2O_5 in wt. %) is a medical grade bioactive glass in clinical use, just as Cerabone-AW® which is an apatite-wollastonite glass-ceramic composed of a mixture of SiO_2 - CaO - B_2O_3 and SiO_2 - CaO - MgO - CaF - P_2O_5 glasses.[5,13] In the clinic, BAGs are mainly applied in particulate form with a size of 90 to 1000 μm, and incorporated in bone defects as stacked particulates or putties. Lower micron to submicron-sized bioactive glass particles are an attractive alternative to the currently clinically implanted micron to millimeter sized granules, as their smaller size results in a higher specific surface area (bioactivity) and makes them well-suited for injection into bone defects or incorporation into composite scaffolds.[15–17]

Much of the pre-clinical research with BAGs has been carried out using large porous bioactive glass scaffolds, either in pure sintered form, or more frequently as polymer-ceramic composites.[18,19] Sintered bioactive glass scaffolds are brittle in nature,[20] and may break down into smaller particles and debris in response to wear, articulation, or mechanical loads experienced *in vivo*.[21,22] Due to increased bioactivity with higher surface-to-volume ratios, BAGs have increasingly been used in particulate form either directly applied to defect sites or combined with polymers to create bioactive composites. Composite scaffolds, such as those created using 3D printing or polymer-filler blending techniques, typically consist of BAG particles homogenously distributed within a polymer matrix.[17,23] The biodegradable nature of these materials raises the likelihood of fine BAG particles being released *in vivo*, potentiating the need to investigate the cellular response to such BAG particles.[16] To date, there is a lack of studies that use clinically relevant human mesenchymal stromal cell (hMSC) to investigate the influence of micron-sized (monodispersed) bioactive glass particles and their ionic dissolution products on cell behavior. This is especially relevant nowadays because of the ever increasing applications of degradable BAGs and their compositional variants in biological settings intending to regenerate bone and soft tissue defects.[24]

The aim of this study was to evaluate the effects of two types of BAGs in different presentation modes on hMSC behavior. Due to their widespread use in marketed medical devices, and wide use in tissue engineering studies, 45S5 and 1393 (53 SiO_2-20 CaO-6 Na_2O-4 P_2O_5-12 K_2O- 5 MgO in wt. %) bioactive glass particles were tested. Both have a track record of stimulating *in vitro* and *in vivo* osteogenesis.[4,25] However, there is only limited previous work in which the biological activity of the two BAGs has been directly compared. In this study, we assessed hMSC metabolic activity, cell spreading, and proliferation capacity when cultured for up to 1 week in direct contact with BAG particles, and compared this to cells exposed to only the BAG dissolution products. Furthermore, we studied the interaction of BAG particles with hydrogel encapsulated hMSCs, thereby providing insights that may be highly relevant for 3D tissue engineering strategies. It is known how ion release influences cell behavior and function, but we hypothesized that local cell populations might additionally physically interact with the implanted BAG particles and respond differently than to mere ionic stimuli. From a clinical translational perspective it would be equally beneficial to investigate the effects of direct physical interactions between BAGs and hMSCs, and with hMSCs cultured in 3D environments. This is the first study to look in-depth in a comparative matter into the cellular behavior of primary hMSCs exposed directly and indirectly to lower micron-sized bioactive glass particles.

MATERIALS AND METHODS

Bioactive glass particles

45S5 BAG particles were obtained from Schott Glass AG (Mainz, Germany), while 1393 BAG particles were obtained by fabricating the bioglass as previously described in,[26] and subsequently crushing and sieving to obtain microparticles.

Cell culture—2D

Human MSCs were isolated from washouts of the femoral bone marrow of a male patient who underwent hip replacement surgery, and characterized as described previously in.[27] Cells were cultured at 37°C in 5% CO_2 atmosphere in Dulbecco's modified Eagle's medium (DMEM, low glucose) (Sigma Aldrich, St. Louis, MO) supplemented with 10 v/v % fetal calf serum (Biochrom AG, Berlin, Germany), 1 v/v % penicillin/streptomycin (Biochrom), and 1 v/v % GlutaMAX™ (Thermo Fischer Scientific, Waltham, MA). Cells were passaged at 70–80% confluence and passages 3–4 were used for all the experiments. Cells were seeded at a density of 5000 cells/well in a 24-well plate in 0.5 mL expansion medium.

Cell culture—3D

Equal amounts of MVG (medium viscosity, high guluronic acid) and LVG (low viscosity, high guluronic acid) ultrapure alginate (Novamatrix, Oslo, Norway) were dissolved in distilled water to a concentration of 1 w/v %, and covalently coupled with the integrin-binding peptide $(Gly)_4$-Arg-Gly-Asp-Ala-Ser-Ser-Lys-Tyr (Peptide 2.0, Chantilly, VA) at 10 peptide molecules per alginate chain using carbodiimide chemistry, as described previously in.[28] Following dialysis, sterile filtration and freez-drying, the modified alginate was reconstituted in serum-free DMEM overnight and mixed with the cell suspension to yield a homogenous mixture of 2 w/v % alginate containing 1.5×10^6 cells/mL. The alginate-cell suspension was extruded through a 30 Gauge needle using a syringe pump (Harvard Apparatus, Holliston, MA) at a constant rate of 0.25 mL/min and collected in a 100 mM $CaCl_2$ bath with constant stirring. After 10 min of crosslinking, alginate beads were retrieved and washed with DMEM to remove excess calcium. Beads were transferred to a 24 well-plate, 2 beads per well in 0.5 mL expansion medium.

Exposure to bioactive glass

Prior to introduction to the cell culture, 45S5 and 1393 BAG particles were passivated for 24 h in serum free DMEM in a

concentration of 5 mg/mL at 37°C. Following centrifugation, the BAG particles were resuspended in cell expansion media to 2.5 w/v %, vortexed to break the BAG agglomerates and further diluted in expansion medium to 0.1, 0.5, 1, and 2.5 w/v %. 0.5 mL of each dilution was added directly to the cell cultures or, in the case of the indirect BAG exposure, in a Transwell® insert (6.5 mm Transwell® with 0.4 μm pore polycarbonate membrane) (Corning, New York, NY) placed in the wells of the 24-well plate.

Ion release from BAG microparticles

To evaluate ion release from BAG microparticles, supernatants from milli-Q water containing 2.5 w/v % of prepassivated 1393 and 45S5 BAGs were collected at different time points (1, 4, and 7 days). Water was used to avoid background interference of various common ions present in buffered solutions such as phosphate buffered solution (PBS). The supernatants were centrifuged and filtered through a 0.22 μm filter to remove debris. The quantification of dissolved Si, Ca, Na, P, K, and Mg in the collected supernatants was done by inductively coupled plasma optical emission spectroscopy (ICP-OES) using an Optima 8300 (Perkin Elmer, USA). For the ICP-OES analyses, six point calibrations (100, 50, 25, 10, 5, and 1 ppm) were performed for all above mentioned elements by diluting certified standards (1000 mg/L, Carl Roth, Germany).

Evaluation of metabolic activity and cell proliferation

The metabolic activity of the hMSCs was analyzed 1, 4, and 7 days after introduction of the BAG particles to the cell culture using the Alamar Blue assay (Biozol, Echingen, Germany). Briefly, BAG and media were removed and replaced with 0.5 mL Alamar Blue master mix (1:10 dilution in cell expansion media). After 2 h incubation at 37°C, 0.1 mL reaction medium from each well was transferred to an opaque 96-well plate and the fluorescence intensity was measured using a spectrophotometer (InfiniteM200Pro, Tecan, Männedorf, Switzerland) with excitation at 530 nm and emission detection at 590 nm.

Following metabolic activity analysis the Alamar Blue solution was removed from the cells cultured on tissue culture plastic (TCP), thoroughly rinsed with dPBS, and frozen at −80°C for DNA quantification. The CyQUANT cell proliferation assay kit (Thermo Fischer Scientific) was used to determine the DNA content. Following the manufacturer's instructions, cell cultures were thawed to room temperature and 0.3 mL CyQUANT® solution was introduced per well and incubated for 5 min. Fluorescence was recorded at an excitation λ of 480 nm and an emission λ of 520 nm using the spectrophotometer.

For 3D cultured cells, the alginate beads were washed with dPBS and alginate was dissociated in 50 mM EDTA solution for 30 min. Following centrifugation, the obtained cell pellet was resuspended and cell number quantified using a C-Chip hemocytometer (NanoEnTek, Seoul, Korea).

All values for metabolic activity and cell numbers were normalized to the positive control (without bioglass addition) at each evaluation time point.

Cell viability staining

The viability and distribution of MSCs inside the alginate beads were evaluated using a Live/Dead cell staining solution. Briefly, alginate beads were washed with calcium free PBS, and incubated for 10 min at 37°C with 0.2 mL cell expansion media containing calcein AM (1:1000) and propidium iodide (1:2500). Encapsulated cells were imaged using an inverted fluorescent microscope (DMI6000B, Leica, Wetzlar, Germany). To quantify cell viability, beads were dissociated by incubation in 50 mM EDTA and the released cells were pelleted, and resuspended in a mixture of calcein AM and propidium iodide. Several images taken from each group were used to quantify the percentage of live and dead cells.

Cell surface area

Cell spreading at 1 and 4 days post-BAG introduction was visualized by staining the actin filaments in the cell body with Alexa Fluor® 488 Phalloidin (Thermo Fischer Scientific) and the cell nucleus with DAPI (Thermo Fischer Scientific). Cells were fixed in 4% neutral buffered formalin for 10 min, washed, and membrane permeabilized with 0.1 v/v % Triton X-100. The cells were then incubated with the staining solution (DAPI (1:1000) and Phalloidin (1:40)) for 20 min at room temperature. Images of stained cells were taken with an inverted fluorescent microscope. The cell surface area of the hMSCs under the different conditions was quantified using Fiji ImageJ software.

Bioactive glass particle size distribution

SEM images were obtained using a Jeol JCM-6000PLUS NeoScope Benchtop SEM (Jeol, Tokyo, Japan) operating at an accelerating voltage of 5 kV, under high vacuum. A magnification of 750× was used. Using Fiji ImageJ software the average BAG particle diameter was determined. The longest side of at least 170 particulates was measured.

Statistics

Unless otherwise stated, all data are represented as mean ± SD. All statistical analyses were performed with GraphPad Prism software 7.0 (GraphPad Software Inc., USA), and statistical significance levels were set at $p < 0.05$ (*), $p < 0.01$ (**), and $p < 0.001$ (***). The Shapiro-Wilk test was used to test for normality. For non-normally distributed data, the Mann-Whitney *U* test (2 groups) or the Kruskal-Wallis with Tukey's *post-hoc* test (>2 groups) was employed. The parametric two-tailed Student's *t* test (2 groups) or one-way ANOVA with Tukey's *post-hoc* test (>2 groups) was used to compare between the two BAG types at similar concentrations, and the same BAG type at different concentrations, respectively. Detailed information about error bars, sample sizes per group, and statistical analyses employed are included in the figure legends.

RESULTS

In this study, three different experimental setups were employed (Fig. 1) to investigate how the mode of interaction (2D direct contact, 2D indirect co-culture, and indirect

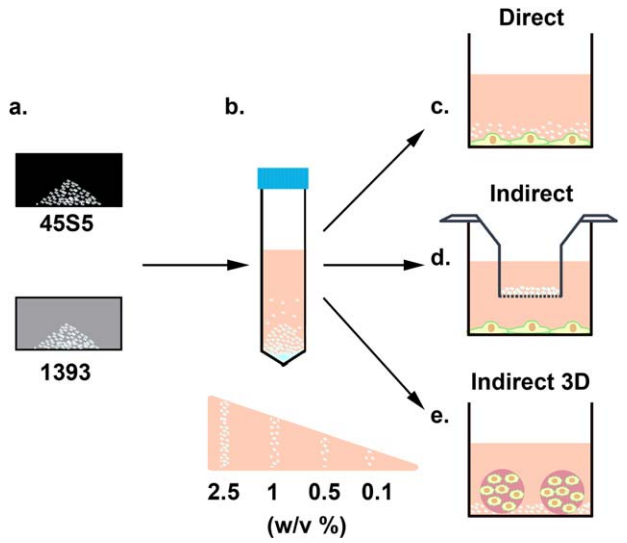

FIGURE 1. Schematic representation of the experimental set-up. (a) 45S5 bioglass® and 1393 bioactive glass particles were (b) suspended in culture medium in different concentrations ranging from 2.5 to 0.1 w/v %. 0.5 mL of the bioactive glass suspension was introduced (c) directly to hMSCs cultured in well plates, (d) indirectly to hMSCs via retention in a 0.4 μm pore size transwell insert, or (e) indirectly to hMSCs encapsulated in 3D alginate beads.

co-culture with 3D encapsulated cells) influenced the biological effects of the 45S5 and 1393 BAG particles on hMSC behavior.

Bioactive glass particle characteristics and ion release

SEM images of BAG particle suspensions [Fig. 2 (a,b)] were used to quantify the particle size distribution [Fig. 2(c)]. The 45S5 BAG particles showed a narrow size distribution with the majority of the particles lying between 3 and 5 μm (mean = 3.6 ± 0.8 μm), whereas most of the 1393 BAG particles had a size range between 3.5 and 5.5 μm (mean = 4.8 ± 1.6 μm), with a maximum of 10 μm. Compositionally well-defined BAGs were used in this study without any additional dopant elements [Fig. 2(d)]. When compared with 45S5, 1393 BAG has a higher SiO_2 content and contains the additional network modifiers K_2O and MgO.

Ion release of Silicon (Si), Magnesium (Mg), Phosphorous (P), Potassium (K), Sodium (Na), and Calcium (Ca) from the BAGs over one week were determined using ICP-OES, and the cumulative release profiles are shown in Figure 3. Despite the lower compositional concentration of CaO in 1393 BAG, calcium ion release was found to be swifter and in greater concentrations compared to 45S5 BAG microparticles. 45S5 BAGs showed a faster release rate of Na and P ions compared to 1393 BAGs, but the cumulative release of P ions over 7 days was below 20 ppm. No difference in Si ion release concentrations or rates were observed between the two BAG types. A constant release of K and Mg ions from 1393 BAG microparticles was observed over the study duration.

Effect of bioactive glass particles on hMSCs behavior (direct contact)

The metabolic activity of hMSCs was negatively affected by the addition of 45S5 or 1393 glass particles, and correlated inversely with increasing glass concentrations (0.1 w/v %–2.5 w/v %) at each evaluation time point [Fig 4(a)]. Strikingly, at all observation time points, the metabolic activity of hMSCs was significantly higher when cultured in the presence of higher concentrations (0.5 w/v % and higher) of 1393 glass particles compared with 45S5 particles. For example at days 4 and 7, exposure to 1 w/v % of 45S5 particles reduced hMSC metabolic activity to <1% of the control cultures, whereas the corresponding values for the 1393 group were ~30% of the control.

To assess the influence of glass particles on hMSC proliferation over time, the DNA content was quantified using the CyQUANT® proliferation assay. Similar to metabolic activity, proliferation was negatively influenced by increasing concentrations of 45S5 or 1393 glass particles [Fig 4(b)]. The addition of either type of bioactive glass did not enhance the proliferation relative to the control; except on day 7, when a significantly increased hMSC proliferation was observed in the presence of 0.1 w/v % 45S5 particles. Despite this overall reduction in cell count, significantly higher cell numbers were detected in all 1393 groups compared to 45S5 groups at similar particle concentrations.

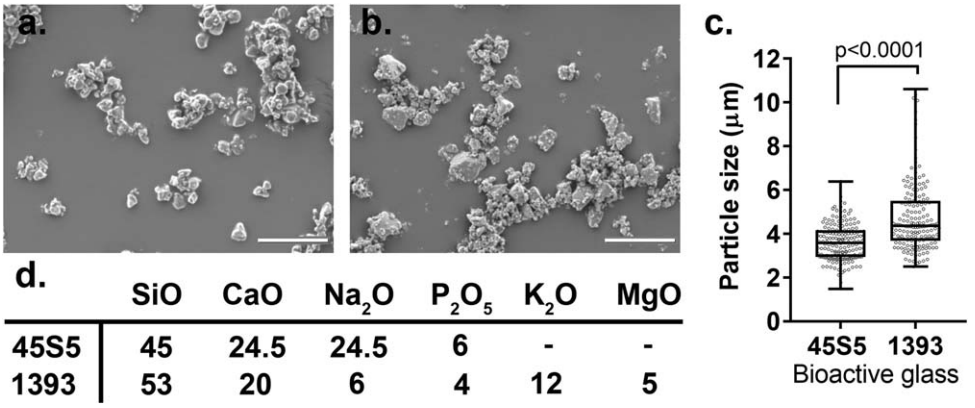

d.

	SiO	CaO	Na_2O	P_2O_5	K_2O	MgO
45S5	45	24.5	24.5	6	-	-
1393	53	20	6	4	12	5

FIGURE 2. Characterization of the bioactive glass particles. SEM images of (a) 45S5 bioglass® particles, and (b) 1393 BAGs. (c) Particle size distribution, measured for the longest side of the particle (n = 170). (d) Composition (wt. %) of 45S5 and 1393 BAGs used in this study. Scale bar: 20 μm.

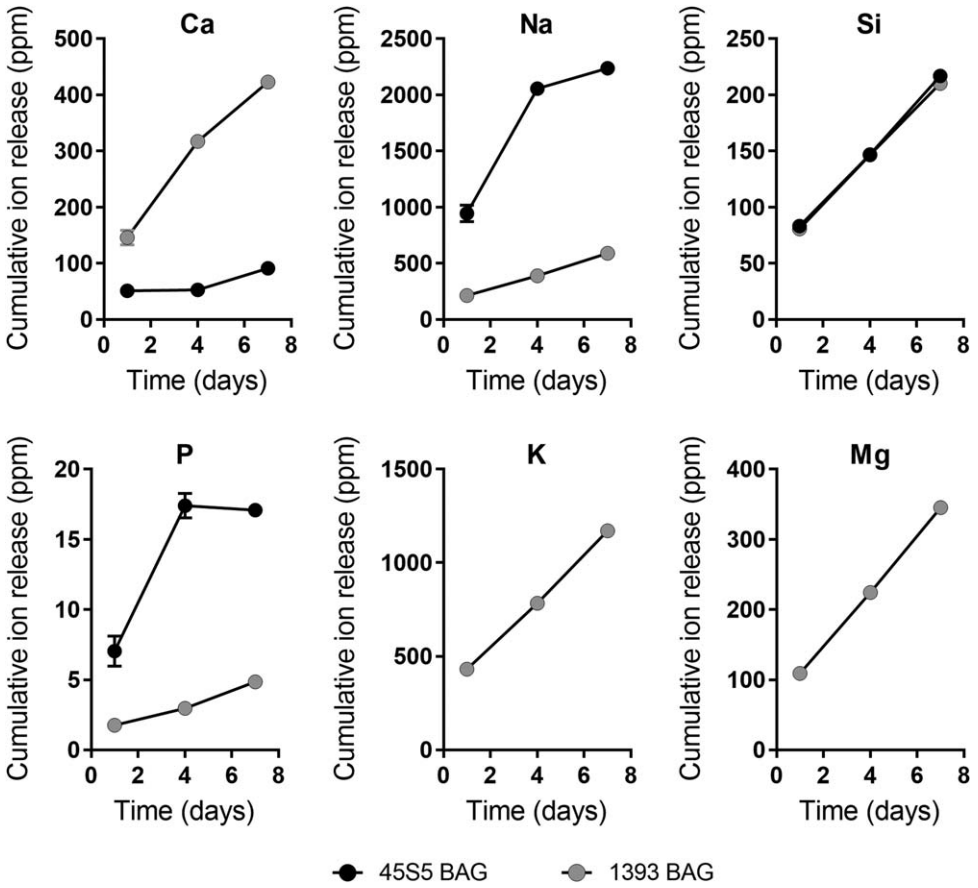

FIGURE 3. Cumulative release profiles of Ca, Na, P, K, Mg, and Si ions from 2.5% w/v of 1393 and 45S5 BAG microparticles over a seven day time period ($n = 3$ per time point).

Interestingly, we noted that despite being significantly less metabolically active, hMSCs exposed to 2.5 w/v % 45S5 BAG had a significantly higher DNA content on day 1 compared with 1393 BAG. Additionally, low amounts of DNA were detected in groups where hMSCs showed zero metabolic activity for example, after exposure to 1 and 2.5 w/v % of 45S5 particles on days 4 and 7. Therefore, the metabolic activity per cell number was analyzed as a more meaningful read out of the cell's metabolic status [Fig. 4(c)]. The data revealed no difference in hMSC metabolic status between 45S5 and 1393 groups at lower BAG concentrations (0.1–0.5 w/v %) at the early time points. However, at higher concentrations, hMSCs had significantly enhanced metabolic status in the presence of 1393 particles compared to 45S5 particles. Increasing the concentration of 45S5 particles had a more pronounced adverse effect on the metabolic status of hMSCs, whereas this was not the case for 1393 particles except at the highest concentration.

To determine whether hMSCs altered their morphology in the presence of BAG particles cell spreading was visualized by phalloidin and DAPI staining and spreading areas were quantified. Qualitatively, cells became less spread, even rounded, with increase in 45S5 concentrations, whereas well-spread cells were detected in the presence of all 1393 concentrations [Fig. 4(d)]. Quantification of the cell area revealed that at each BAG concentration, hMSCs in the presence of 1393 particles had a significantly higher coverage area compared to cells in the presence of 45S5 particles [Fig 4(e)]. Strikingly, cell area decreased from ~3300 to <100 μm^2 when the concentration of added 45S5 particles increased from 0.1 w/v % to 2.5 w/v %, whereas over the same concentration range of 1393 particles, cell area only marginally changed from ~4900 to ~4700 μm^2.

Effect of bioactive glass dissolution products on hMSCs behavior (indirect contact)

To investigate whether the negative influence of BAG particles on cell behavior was caused by the physical or ionic interaction between glass particles and the hMSCs, the experiments were extended to BAG delivery via porous transwell inserts in the hMSC cultures. This set-up prevented particle leakage and hence direct BAG-cell contact, but allowed ionic release into the shared culture medium.

A reduction in the metabolic activity of hMSCs was evident with increasing BAG concentrations, but it was less pronounced for 1393 release products [Fig. 5(a)]. Contrary to what was observed in the direct contact set-up, increasing concentrations of 1393 release products did not negatively influence hMSC metabolic activity. At all tested time points, hMSC metabolic activity remained above 70% of the

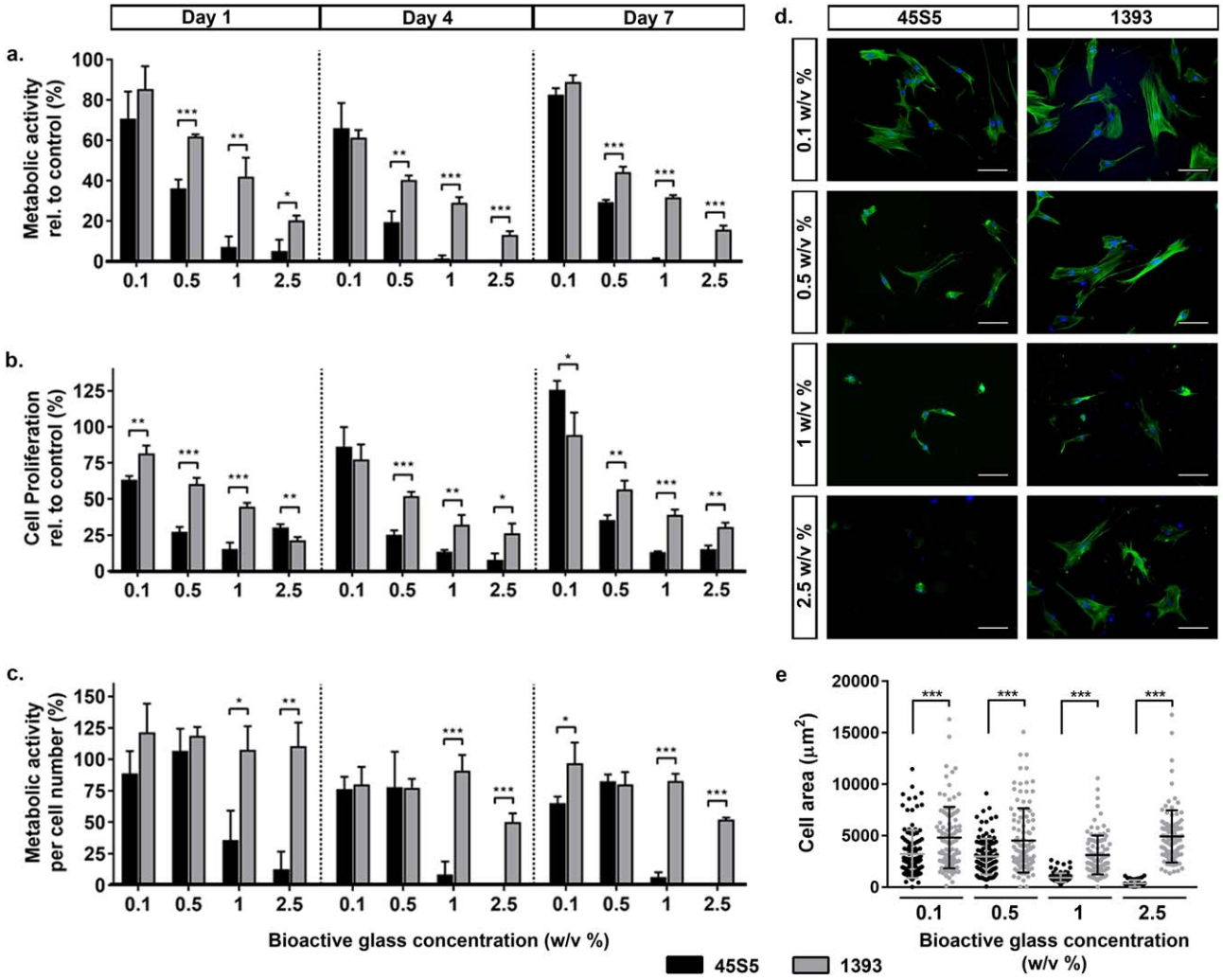

FIGURE 4. Effect of 45S5 and 1393 bioactive glass particles on hMSC behavior (direct contact). (a) Metabolic activity of hMSCs in direct contact with different concentrations (0.1, 0.5, 1, and 2.5 w/v %) of 45S5 (black bars) and 1393 (gray bars) BAGs relative to control non-supplemented cell cultures at days 1, 4, and 7. (b) Proliferation of hMSCs cultured with the different concentrations of BAGs relative to the control cultures, determined by DNA quantification. (c) Metabolic activity of the hMSCs normalized to cell number. (d) Representative day 1 images of hMSCs in direct contact with 45S5 and 1393 BAGs, stained for actin cytoskeleton (green: Alexa Fluor® 488 Phalloidin) and cell nucleus (blue: DAPI). (e) Quantification of cell spreading area of hMSCs after 1 day of direct culture with different bioactive glass [$n = 40–100$].Statistical significance levels were set at $p < 0.05$ (*), $p < 0.01$ (**), and $p < 0.001$ (***), scale bar: 100 μm.

control in the 1393 BAG groups. Moreover, at higher concentrations (1–2.5 w/v %), hMSC metabolic activity was significantly greater in the presence of 1393 release products compared with 45S5 release products. At these concentrations, the metabolic activity of 2D/TCP cultured hMSCs in indirect contact was higher than when the cells were in physical contact to either of the two BAG compositions (Supporting Information Fig. S1). Once again, exposure to ionic release products from either BAGs did not considerably enhance hMSC metabolic activity compared with the control.

Similar trends were observed for cell proliferation [Fig 5(b)]. Cell numbers were starkly reduced (by ~40%) as the 45S5 BAG concentration was increased from 1 to 2.5 w/v %. This sharp decrease was not observed for hMSCs exposed to 1393 BAG. After 7 days of culture, similar cell numbers were observed in all wells irrespective of 1393 BAG concentration. At the two highest concentrations (1–2.5 w/v %), significantly greater cell numbers were detected in the 1393 groups compared with the 45S5 groups.

Quantification of the metabolic activity per cell number revealed counter-intuitive results, especially at the day 7 time point [Fig. 5(c)]. Contrary to the results of the direct contact setup, indirect co-culture did not negatively influence the metabolic status of hMSCs, even at higher concentrations. At days 1 and 4, no differences in metabolic status existed between hMSCs that were exposed to 45S5 or 1393 release products. After 7 days of co-culture, the metabolic status of hMSCs in all BAG groups was significantly higher than the non-supplemented control, and cells were significantly more metabolically active in the presence of 45S5 BAG compared to 1393 BAG.

Fluorescent images indicated that hMSCs were well spread with prominent actin fibers in all groups, except at

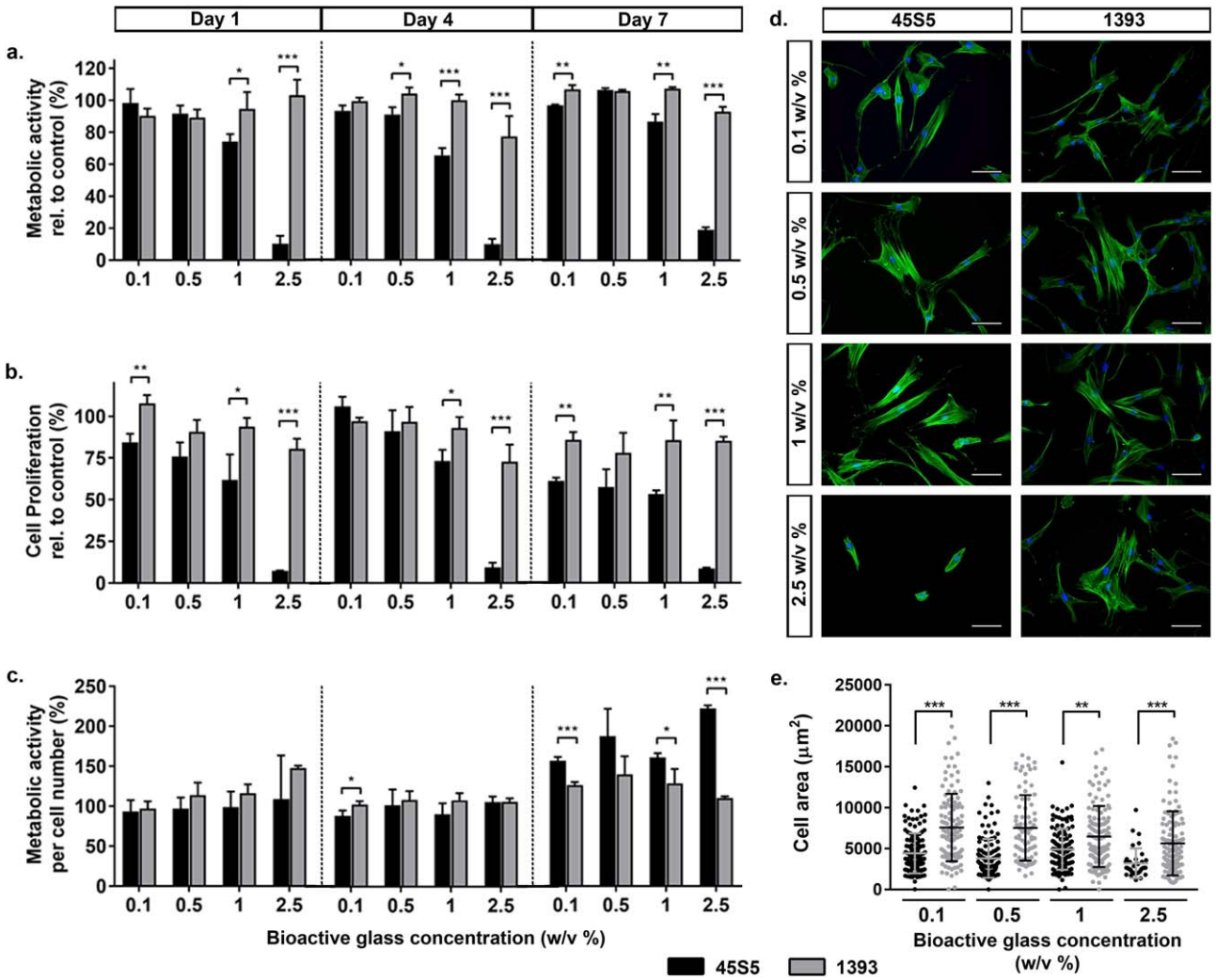

FIGURE 5. Effect of 45S5 and 1393 bioactive glass dissolution products on hMSC behavior (indirect contact). (a) Metabolic activity of hMSCs exposed to the dissolution products of different concentrations (0.1, 0.5, 1, and 2.5 w/v %) of 45S5 (black bars) and 1393 (grey bars) BAGs relative to control non-supplemented cell cultures at days 1, 4, and 7. (b) Proliferation of hMSCs cultured with the dissolution products of different concentrations of BAGs relative to the control cultures. (c) Metabolic activity of the hMSCs normalized to cell number. (d) Representative day 1 images of hMSCs indirectly exposed to 45S5 and 1393 BAGs, stained for actin cytoskeleton (green: Alexa Fluor® 488 Phalloidin) and cell nucleus (blue: DAPI). (e) Quantification of cell spreading area of hMSCs after one day of indirect exposure to different bioactive glass concentrations [$n = 34$–100]. Statistical significance levels were set at $p < 0.05$ (*), $p < 0.01$ (**), and $p < 0.001$ (***), scale bar: 100 μm.

the highest concentration of 45S5 BAG, where cells were visibly less spread [Fig. 5(d)]. Quantification of cell area highlighted the significantly greater spreading in the presence of dissolution ions of 1393 BAG compared with 45S5 BAG at all concentrations [Fig 5(e)]. With increase in 45S5 BAG concentrations, the cell area decreased from ~4500 μm^2 (0.1 w/v %) to ~3100 μm^2 (2.5 w/v %). For 1393 BAG, the cell area decreased from ~7500 (0.1 w/v %) to ~5500 μm^2 (2.5 w/v %).

Effect of bioactive glass dissolution products on hydrogel encapsulated hMSCs (indirect 3D)

Next, we investigated the effects of 45S5 and 1393 BAG on the behavior of hMSCs in 3D culture conditions. To implement this, hMSCs were encapsulated in cell-interactive alginate beads via calcium mediated ionic crosslinking. The cells were primarily exposed to the dissolution products of the BAGs in this set-up as well.

The metabolic activity of encapsulated cells drastically decreased with increasing 45S5 BAG concentration at all evaluation time points [Fig. 6(a)]. In contrast, 1393 BAG did not alter the metabolic activity of the 3D cultured cells as strongly. For instance, at 2.5 w/v % of 45S5 BAG particles, no metabolic activity was detected at days 1 and 7, whereas for the same concentration of 1393 BAG particles, cells exhibited >60% metabolic activity relative to the control. Furthermore, hMSC metabolic activity was significantly higher in the presence of 1393 BAG particles compared with 45S5 BAG particles, especially at higher concentrations (1–2.5 w/v %). At these concentrations, it was apparent that cells cultured on TCP in indirect contact to either of the tested BAGs exhibited a higher metabolic activity than

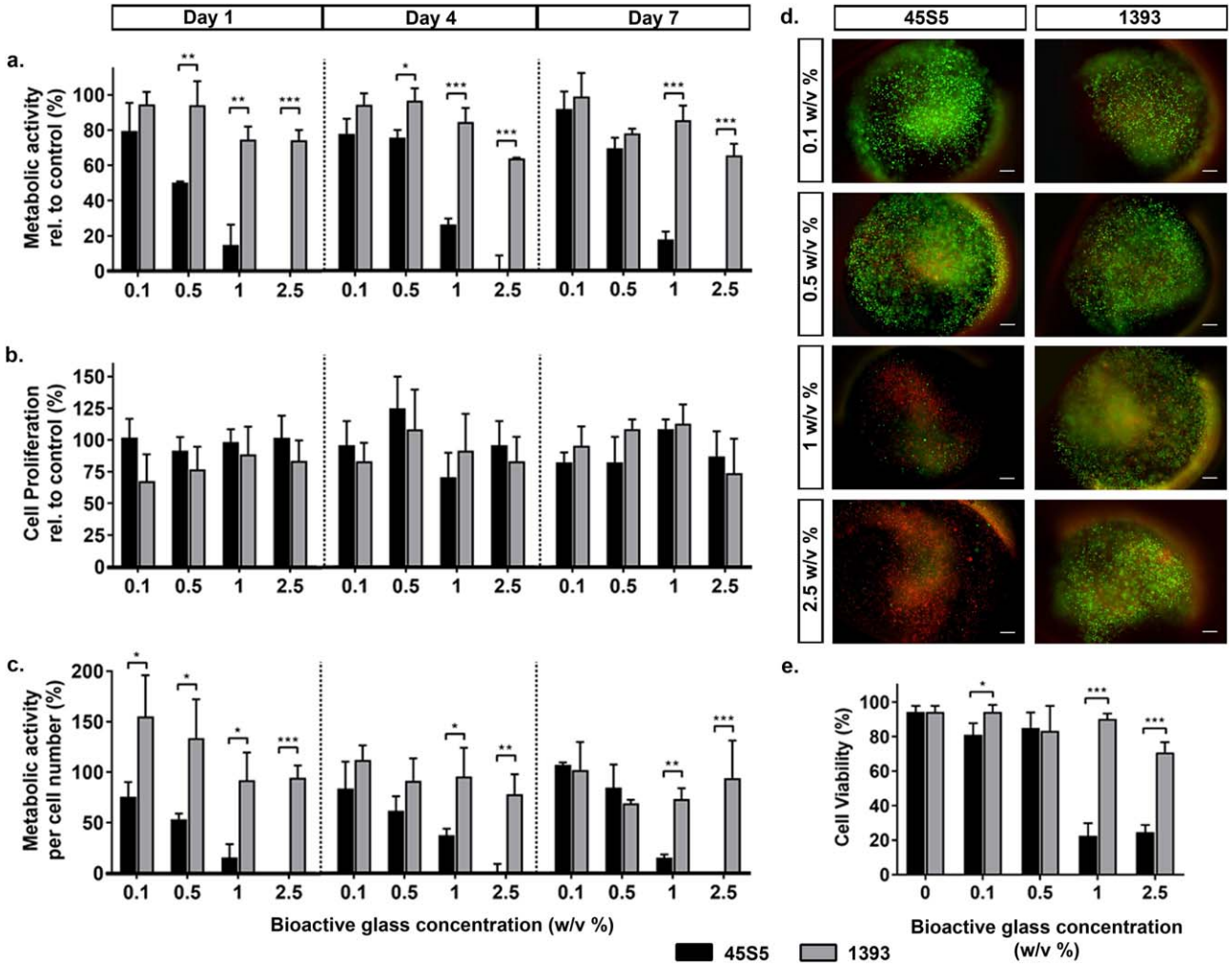

FIGURE 6. Effect of 45S5 and 1393 bioactive glass dissolution products on alginate encapsulated hMSCs (indirect 3D). (a) Metabolic activity of encapsulated hMSCs cultured in medium containing different concentrations (0.1, 0.5, 1, and 2.5 w/v %) of 45S5 (black bars) and 1393 (gray bars) BAGs relative to control non-supplemented encapsulated cell cultures at days 1, 4, and 7. (b) Proliferation of encapsulated cells after culture with different concentrations of BAGs relative to the control cultures, as determined by alginate dissolution and subsequent cell counting. (c) Metabolic activity of the hMSCs normalized to cell number. (d) Representative day 1 images of encapsulated hMSCs cultured with 45S5 and 1393 BAGs, stained for live (green: calcein AM) and dead (red: propidium iodide) cells. (e) Quantification of cell viability after one day of culture. Statistical significance levels were set at $p < 0.05$ (*), $p < 0.01$ (**), and $p < 0.001$ (***), scale bar: 200 μm.

when they were cultured in a 3D hydrogel environment (Supporting Information Fig. S1).

Analysis of cell proliferation suggested that cell numbers remained consistent over time in all tested groups, and that this was similar to values obtained for the control samples, indicating that the beads efficiently encapsulated the cells over the time course of the experiment [Fig. 6(b)]. The presence of 1393 BAG particles led to a significantly higher metabolic status of encapsulated hMSCs in comparison to 45S5 BAG particles, which showed a negative correlation with increasing BAG concentration [Fig 6(c)].

Although encapsulated, cells maintained a rounded morphology due to the rigidity of the hydrogel matrix which prevented cell spreading and movement (data not shown). Figure 6(d) shows representative images of alginate beads containing hMSCs stained with calcein AM (green = live cells), and propidium iodide (red = dead cells). The corresponding quantification of encapsulated cell viability is shown in Figure 6(e). hMSCs remained highly viable in the presence of up to 0.5 w/v % of 45S5 or 1393 BAG particles. At higher concentrations (1–2.5 w/v %) of 45S5 BAG particles however, the viability dropped to ~20% confirming the large amount of propidium iodide stained cells observed in the hydrogel. However, at similar concentrations of 1393 BAG particles, the cells maintained a viability of at least 70%, confirming the largely green calcein positive stained cells observed during imaging. These results demonstrate that in 3D culture conditions, 45S5 BAG concentrations of >0.5 w/v % are detrimental to cell viability and function, whereas even higher concentrations of 1393 BAG do not cause adverse effects on cell viability or function.

DISCUSSION

In this study, we investigated the effect of micron sized particles of 45S5 and 1393 BAGs and their ionic dissolution

products on hMSC behavior. The outcomes revealed that basic cellular functions such as metabolic activity, proliferation, and cell spreading can vary largely depending on the concentration and type of bioactive glass, as well as the mode of interaction between hMSCs and the BAG particles.

The 45S5 BAG used in this study is the BAG originally reported by Hench,[1] which has subsequently been commercialized for bone grafting procedures.[29] From a clinical perspective, synthetic graft materials in the form of particulates and granules are preferred because they can be mixed with biological fluids such as blood and compacted into the quite often irregularly shaped defect sites during implantation.[30] Therefore, most of the bioactive glass based products are marketed as granules in the 90–1000 μm size range.[31] Recent research efforts have involved the incorporation of BAG particles into polymer based composites to exploit the improved bioactivity associated with high surface-to volume-ratios of micron and sub-micron sized particles.[32] BAG granules as well as BAG containing composites not only release cell stimulating ions, but are also likely to break down into smaller micro- and nano-particle debris which can interact with cells present in the local biological milieu. Although a number of studies have highlighted the beneficial effects of bioactive glass dissolution products, often in a conditioned media setting, the influence of particle contact on relevant cells such as MSCs remains unexplored.

Hence, the direct contact setup employed in this study aimed to investigate how hMSC behavior is influenced by the physical interaction with bioactive glass particles. The results demonstrate that basic cellular functions such as metabolic activity, proliferation, and cell spreading were adversely affected by higher concentrations of the BAGs. To decouple the physical and chemical effects of the BAG particles, we used transwell inserts to prevent direct cell–particle interaction but permit cell interaction with BAG dissolution products. In comparison to the direct setup, hMSCs showed much higher metabolic activities and proliferation when physical contact with BAG particles was prevented. Despite the change in interaction mode, the highest concentration of 45S5 BAG particles had a considerable negative influence on hMSC metabolic activity and proliferation. The higher concentrations were included in the study because they are more likely to induce desirable bioactive (hydroxyapatite formation), osteogenic, angiogenic, and anti-microbial effects.[33,34] Moreover, in a clinical setting, smaller voids and defects are often completely filled with bioactive graft materials, which results in high, local concentrations of the material. Host cell populations from the surrounding tissue (e.g. bone marrow or periosteum) are expected to migrate into the graft material, attach and proliferate to induce a regenerative outcome.[35] That this cell-material interaction may be more complex (physical interaction vs. ionic interaction, low concentration vs. high concentration) is apparent from our results. In agreement with our observations, previously published reports indicate negative effects on cell viability and proliferation in response to high BAG concentrations.[15,36] Interestingly, we observed that at almost all tested concentrations, 1393 bioactive glass particles showed better effects on hMSC behavior over 45S5 particles. This difference was clearly evident from the morphological analysis of the cultured hMSCs, which showed significantly higher cell spreading in the presence of 1393 BAG particles compared with 45S5 particles. Increased cell spreading with filopodial extensions is indicative of cells probing their surrounding environment, whereas cell rounding and blebbing have been linked to increased cellular stress and a transition to cell death.[37,38] Based on SEM analysis, the two bioactive glass particles used in this study had a size range of 3–8 μm with narrow size distributions, making it less likely that the differences in hMSC functional behavior between 45S5 versus1393 BAGs was caused by differences in surface roughness or internalization of the particles.[39] It is more probable that the observed effects were caused by the differences in BAG ion release. For instance, despite containing a higher concentration of CaO (24.5 vs. 20%), rapid and significantly higher release of Ca ions was observed from 1393 BAG particles. The highest absolute concentrations were recorded for sodium ions from 45S5 BAG microparticles (∼2200 ppm over 7 days), which was ∼ 3-fold higher than the concentrations recorded from 1393 BAG microparticles (∼550 ppm over 7 days). The ion release profiles in this study were obtained from experiments conducted in high purity water, and may vary slightly if the study is conducted using culture medium or carried out *in vivo*. These ion release trends were in agreement with those reported previously in literature for BAG-based scaffolds.[26,40] Contrary to 45S5 BAG, 1393 BAG is composed of additional K^+ and Mg^{2+} ions. Previous studies have already reported on the positive effects of magnesium ions on cell viability, proliferation, and spreading.[41] Furthermore, it is well documented that hMSCs express cationic channels on their cell membrane and that K^+, Na^+, and Ca^{2+} channels are involved in cell proliferation, migration and differentiation.[42,43] The blocking of Na^+ channels, for instance, increases hMSC proliferation, while blocking calcium-activated K^+ channels results in diminished hMSC proliferation.[43] The exact mechanism underlying the regulation of cell proliferation by ion channels remains to be clarified, and is beyond the scope of this study. However, the stark differences in released Ca, Na, and P ions from 1393 and 45S5 BAG particles, together with the potential effects of K and Mg ions from 1393 BAG particles might play a role in promoting more cell proliferation and the better results observed with this type of BAG. Future studies could address this hypothesis by investigating the dose dependent effects of separate ions on MSC behavior and correlating observed effects with ion release profiles from BAG particles.

Since cells *in vivo* are organized in a 3D microenvironment through cell–cell and cell–ECM interactions, it was interesting to investigate the influence of bioactive glass and its dissolution products on 3D cultured hMSCs. To control this 3D environment, hMSCs were encapsulated at high cell densities in an alginate hydrogel functionalized with a well-defined composition of cell interactive integrin binding RGD motifs. The cell encapsulating beads were then co-cultured with BAG microparticles suspended in culture media. Contrary to our initial assumption that the 3D environment would provide an additional protection to the cells, we observed a significant decrease in cell

viability at the two highest tested concentrations of both BAGs. In particular, this effect was most pronounced for the 45S5 BAG conditions, where a significant decrease in cell viability and cell metabolic activity was observed even at the lowest tested concentrations. When cell loaded alginate beads were cultured with the two highest tested 45S5 BAG concentrations, cell function (both metabolic activity and proliferation) dropped below 20% compared with the control cultures in non-BAG-supplemented medium. This observed effect was also apparent in the live/dead staining of the entrapped cells, where the majority of the hMSCs stained positive for propidium iodide, a dye to distinguish dead cells.

Alno et al.[44] reported a similar differential effect of 45S5 BAG ionic dissolution products (1 w/v %–400 μm particle size) on the proliferation of human fetal osteoblasts cultured in 2D versus 3D spheroid culture. While they observed an increase in cell viability at 4 and 7 days for TCP cultured cells in contact with BAG conditioned medium, they report a significant decrease in cell viability for 3D cultured cells.[44] In native adult tissues, the microenvironment is characterized by greater cell–matrix interactions than cell–cell interactions. Therefore, spheroid cultures may not be the optimal set up to investigate BAG–cell interactions in 3D. Moreover, multicellular spheroids can have a hypoxic cluster of cells at their core, which may interfere with cell viability and metabolic activity measurements. These potential issues are avoided in the current system where alginate encapsulated MSCs maintain high viability in non-BAG stimulated conditions. A further practical advantage is the relatively convenient retrieval of the cells from their 3D environment for further single cell characterization.

Contrary to the data for the metabolic activity, the cell proliferation data did not show any significant differences between both BAGs at any of the tested concentrations for the encapsulated cells. This was to be expected since the cell proliferation graph represents the total number of encapsulated cells in the beads and the hydrogel matrix surrounding encapsulated cells does not permit cell spreading or multiplication.

In summary, the data presented here demonstrates that basic cellular responses can vary depending on the composition, concentration, and presentation mode of bioactive glass microparticles. Future work should address how the differentiation, paracrine, and immunomodulatory behavior of MSCs could be influenced by exposure to these BAGs. Additionally, a comparative assessment of the ability of these biomaterials to induce *in vivo* bone formation in an appropriate model of bone injury such as critical size long bone defects would help to validate these *in vitro* findings.

CONCLUSIONS

Taken together, these results show that compared with mere exposure to ionic release products, physical interaction between bioactive glass particles and primary MSCs can differently alter cell metabolic activity, spreading, and proliferation. Furthermore, the composition, and subsequent release kinetics of various ions from different BAG types such as 45S5 and 1393 may play an important role in stimulating these altered cell behaviors. Our study shows that experimental settings that mimic the interaction of local cells to implanted materials may be more informative: (1) cells may be less tolerant to higher concentrations of certain BAG compositions than others when physical interaction takes place (direct contact vs. indirect contact), and (2) cells in a 3D environment may show an enhanced sensitivity to ionic release products than those cultured on TCP substrates (indirect 2D vs. indirect 3D). These outcomes will likely have important implications for the pre-clinical evaluation of promising bioactive materials.

ACKNOWLEDGMENTS

The authors gratefully acknowledge Dr. Sven Geissler for use of fluorescence plate reader and inverted microscope. The cell harvesting unit of the BCRT is acknowledged for providing primary human MSCs. The authors further thank Dr. Katharina Schmidt-Bleek for constructive discussions.

REFERENCES

1. Hench LL, Splinter RJ, Allen WC, Greenlee TK. Bonding mechanisms at the interface of ceramic prosthetic materials. J Biomed Mater Res 1971;5:117–141.
2. Cortez PP, Brito AF, Kapoor S, Correia AF, Atayde LM, Dias-Pereira P, Maurício AC, Afonso A, Goel A, Ferreira JMF. The in vivo performance of an alkali-free bioactive glass for bone grafting, FastOs®BG, assessed with an ovine model. J Biomed Mater Res B Appl Biomater 2017;105:30–38.
3. Fu Q, Rahaman MN, Fu H, Liu X. Silicate, borosilicate, and borate bioactive glass scaffolds with controllable degradation rate for bone tissue engineering applications. I. Preparation and in vitro degradation. J Biomed Mater Res A 2010;95:164–171.
4. Bi L, Jung S, Day D, Neidig K, Dusevich V, Eick D, Bonewald L. Evaluation of bone regeneration, angiogenesis, and hydroxyapatite conversion in critical-sized rat calvarial defects implanted with bioactive glass scaffolds. J Biomed Mater Res A 2012;100:3267–3275.
5. Heikkila JT, Kukkonen J, Aho AJ, Moisander S, Kyyronen T, Mattila K. Bioactive glass granules: a suitable bone substitute material in the operative treatment of depressed lateral tibial plateau fractures: a prospective, randomized 1 year follow-up study. J Mater Sci Mater Med 2011;22:1073–1080.
6. Xynos ID, Edgar AJ, Buttery LD, Hench LL, Polak JM. Gene-expression profiling of human osteoblasts following treatment with the ionic products of Bioglass 45S5 dissolution. J Biomed Mater Res 2001;55:151–157.
7. Zhang W, Zhao F, Huang D, Fu X, Li X, Chen X. Strontium-substituted submicrometer bioactive glasses modulate macrophage responses for improved bone regeneration. ACS Appl Mater Interfaces 2016;8:30747–30758.
8. Tsigkou O, Jones JR, Polak JM, Stevens MM. Differentiation of fetal osteoblasts and formation of mineralized bone nodules by 45S5 Bioglass conditioned medium in the absence of osteogenic supplements. Biomaterials 2009;30:3542–3550.
9. Quinlan E, Partap S, Azevedo MM, Jell G, Stevens MM, O'Brien FJ. Hypoxia-mimicking bioactive glass/collagen glycosaminoglycan composite scaffolds to enhance angiogenesis and bone repair. Biomaterials 2015;52:358–366.
10. Hoppe A, Güldal NS, Boccaccini AR. A review of the biological response to ionic dissolution products from bioactive glasses and glass-ceramics. Biomaterials 2011;32:2757–2774.
11. Gentleman E, Fredholm YC, Jell G, Lotfibakhshaiesh N, O'Donnell MD, Hill RG, Stevens MM. The effects of strontium-substituted bioactive glasses on osteoblasts and osteoclasts in vitro. Biomaterials 2010;31:3949–3956.
12. Popescu RA, Magyari K, Vulpoi A, Trandafir DL, Licarete E, Todea M, Stefan R, Voica C, Vodnar DC, Simon S, and others. Bioactive and biocompatible copper containing glass-ceramics with

remarkable antibacterial properties and high cell viability designed for future in vivo trials. Biomater Sci 2016;4:1252–1265.
13. Hench LL, Jones JR. Bioactive glasses: frontiers and challenges. Front Bioeng Biotechnol 2015;3:194.
14. Vallet-Regí M, Salinas AJ, Arcos D. Tailoring the structure of bioactive glasses: from the nanoscale to macroporous scaffolds. Int J Appl Glass Sci 2016;7:195–205.
15. Tsigkou O, Labbaf S, Stevens MM, Porter AE, Jones JR. Monodispersed bioactive glass submicron particles and their effect on bone marrow and adipose tissue-derived stem cells. Adv Healthc Mater 2014;3:115–125.
16. Vichery C, Nedelec J-M. Bioactive glass nanoparticles: from synthesis to materials design for biomedical applications. Materials 2016;9:288.
17. Rezwan K, Chen QZ, Blaker JJ, Boccaccini AR. Biodegradable and bioactive porous polymer/inorganic composite scaffolds for bone tissue engineering. Biomaterials 2006;27:3413–3431.
18. Kolan KC, Leu MC, Hilmas GE, Brown RF, Velez M. Fabrication of 13–93 bioactive glass scaffolds for bone tissue engineering using indirect selective laser sintering. Biofabrication 2011;3:025004.
19. Lu W, Ji K, Kirkham J, Yan Y, Boccaccini AR, Kellett M, Jin Y, Yang XB. Bone tissue engineering by using a combination of polymer/Bioglass composites with human adipose-derived stem cells. Cell Tissue Res 2014;356:97–107.
20. Bertolla L, Dlouhý I, Philippart A, Boccaccini AR. Mechanical reinforcement of Bioglass®-based scaffolds by novel polyvinyl-alcohol/microfibrillated cellulose composite coating. Mater Lett 2014; 118:204–207.
21. Yang G, Yang X, Zhang L, Lin M, Sun X, Chen X, Gou Z. Counterionic biopolymers-reinforced bioactive glass scaffolds with improved mechanical properties in wet state. Mater Lett 2012;75:80–83.
22. Coathup MJ, Cai Q, Campion C, Buckland T, Blunn GW. The effect of particle size on the osteointegration of injectable silicate-substituted calcium phosphate bone substitute materials. J Biomed Mater Res B Appl Biomater 2013;101:902–910.
23. Luo Y, Wu C, Lode A, Gelinsky M. Hierarchical mesoporous bioactive glass/alginate composite scaffolds fabricated by three-dimensional plotting for bone tissue engineering. Biofabrication 2013;5:015005.
24. Miguez-Pacheco V, Hench LL, Boccaccini AR. Bioactive glasses beyond bone and teeth: emerging applications in contact with soft tissues. Acta Biomater 2015;13:1–15.
25. Fu Q, Rahaman MN, Bal BS, Bonewald LF, Kuroki K, Brown RF. Silicate, borosilicate, and borate bioactive glass scaffolds with controllable degradation rate for bone tissue engineering applications. II. In vitro and in vivo biological evaluation. J Biomed Mater Res A 2010;95:172–179.
26. Hoppe A, Jokic B, Janackovic D, Fey T, Greil P, Romeis S, Schmidt J, Peukert W, Lao J, Jallot E, Boccaccini AR. Cobalt-releasing 1393 bioactive glass-derived scaffolds for bone tissue engineering applications. ACS Appl Mater Interfaces 2014;6:2865–2877.
27. Kasper G, Glaeser JD, Geissler S, Ode A, Tuischer J, Matziolis G, Perka C, Duda GN. Matrix metalloprotease activity is an essential link between mechanical stimulus and mesenchymal stem cell behavior. Stem Cells 2007;25:1985–1994.
28. Rowley JA, Madlambayan G, Mooney DJ. Alginate hydrogels as synthetic extracellular matrix materials. Biomaterials 1999;20: 45–53.
29. Hench LL. Opening paper 2015- some comments on bioglass: four eras of discovery and development. Biomed Glass 2015;1:1–11.
30. Zamet JS, Darbar UR, Griffiths GS, Bulman JS, Bragger U, Burgin W, Newman HN. Particulate bioglass as a grafting material in the treatment of periodontal intrabony defects. J Clin Periodontol 1997;24:410–418.
31. Jones JR. Review of bioactive glass: from Hench to hybrids. Acta Biomater 2013;9:4457–4486.
32. Sarker B, Hum J, Nazhat SN, Boccaccini AR. Combining collagen and bioactive glasses for bone tissue engineering: a review. Adv Healthc Mater 2015;4:176–194.
33. Zhang D, Lepparanta O, Munukka E, Ylanen H, Viljanen MK, Eerola E, Hupa M, Hupa L. Antibacterial effects and dissolution behavior of six bioactive glasses. J Biomed Mater Res A 2010;93: 475–483.
34. Leu A, Leach JK. Proangiogenic potential of a collagen/bioactive glass substrate. Pharm Res 2008;25:1222–1229.
35. Leu A, Stieger SM, Dayton P, Ferrara KW, Leach JK. Angiogenic response to bioactive glass promotes bone healing in an irradiated calvarial defect. Tissue Eng Part A 2009;15:877–885.
36. Rismanchian M, Khodaeian N, Bahramian L, Fathi M, Sadeghi-Aliabadi H. In-vitro comparison of cytotoxicity of two bioactive glasses in micropowder and nanopowder forms. Iran J Pharm Res 2013;12:437–443.
37. Fulda S, Gorman AM, Hori O, Samali A. Cellular stress responses: cell survival and cell death. Int J Cell Biol 2010;2010:23.
38. Chen CS, Mrksich M, Huang S, Whitesides GM, Ingber DE. Geometric control of cell life and death. Science 1997;276:1425–1428.
39. Zan X, Sitasuwan P, Feng S, Wang Q. Effect of roughness on in situ biomineralized cap-collagen coating on the osteogenesis of mesenchymal stem cells. Langmuir 2016;32:1808–1817.
40. Hoppe A, Meszaros R, Stahli C, Romeis S, Schmidt J, Peukert W, Marelli B, Nazhat SN, Wondraczek L, Lao J, and others. In vitro reactivity of Cu doped 45S5 Bioglass[registered sign] derived scaffolds for bone tissue engineering. J Mater Chem B 2013;1: 5659–5674.
41. Cifuentes SC, Bensiamar F, Gallardo-Moreno AM, Osswald TA, Gonzalez-Carrasco JL, Benavente R, Gonzalez-Martin ML, Garcia-Rey E, Vilaboa N, Saldana L. Incorporation of Mg particles into PDLLA regulates mesenchymal stem cell and macrophage responses. J Biomed Mater Res A 2016;104:866–878.
42. Li GR, Sun H, Deng X, Lau CP. Characterization of ionic currents in human mesenchymal stem cells from bone marrow. Stem Cells 2005;23:371–382.
43. Ding F, Zhang G, Liu L, Jiang L, Wang R, Zheng Y, Wang G, Xie M, Duan Y. Involvement of cationic channels in proliferation and migration of human mesenchymal stem cells. Tissue Cell 2012;44: 358–364.
44. Alno N, Jegoux F, Pellen-Mussi P, Tricot-Doleux S, Oudadesse H, Cathelineau G, De Mello G. Development of a three-dimensional model for rapid evaluation of bone substitutes in vitro: Effect of the 45S5 bioglass. J Biomed Mater Res A 2010;95A:137–145.